

# Interaction between Liquid Droplet Growth and Two-Phase Pressure Drop in PEM Fuel Cell Flow Channels

Mehdi Mortazavi<sup>1</sup>, Kazuya Tajiri<sup>2</sup>

<sup>1</sup>Multiscale Thermal Fluids Laboratory, Western New England University  
1215 Wilbraham Road, Springfield, MA 01119, USA  
mehdi.mortazavi@wne.edu

<sup>2</sup>Multiscale Transport Process Laboratory, Michigan Technological University  
1400 Townsend Drive, Houghton, MI 49931, USA  
ktajiri@mtu.edu

**Abstract** - In this paper, liquid-gas two-phase flow pressure drop in proton exchange membrane (PEM) fuel cell is studied in an ex-situ experimental setup. The two-phase flow pressure drop is measured during liquid water droplet emergence and growth on the surface of the gas diffusion layer (GDL). The two-phase flow pressure measurement is synchronized with a high speed camera that records droplet emergence and growth. Simultaneous study of droplet size and liquid-gas two-phase flow pressure drop reveals useful information which can be utilized in analyzing existing two-phase flow pressure drop models.

**Keywords:** PEM fuel cell, two-phase flow, pressure drop, droplet

## 1. Introduction

Proton exchange membrane (PEM) fuel cells are an efficient and pollutant free type of energy system that can provide power for different applications [1,2]. As the electrochemical reactions occur within the cell, hydrogen and oxygen are utilized to generate electricity. Such reactions have water and heat as their byproducts. The gas diffusion layer (GDL) is a porous layer inserted between flow channels and catalyst layer. GDL has different roles including distributing reactant gases over catalyst layers and transporting produced water in catalyst layer to the flow channels. The water produced in an operating PEM fuel cell can fill the open pores of the GDL which eventually blocks the transport of reactant gases to the catalyst layer. This phenomenon is referred to as GDL flooding and has been reported to significantly lower the performance of the cell [3,4,5]. A reliable fuel cell performance requires an uniform and continuous supply of reactants to the electrodes. This can be achieved by acquiring an accurate knowledge about the liquid water interaction with gas species within the gas channel and porous layers.

During the operation of a PEM fuel cell, liquid water may emerge from the surface of the GDL at some preferential locations [6] and enter the gas channel. This causes liquid-gas two-phase flow within the gas channel. When water removal rate is less than water production rate, liquid water accumulates in gas channel and eventually causes channel flooding. Similar to GDL flooding, channel flooding has been reported to lower the performance of the cell [7,8].

Liquid-gas two-phase flow in PEM fuel cell flow channels can be studied by direct and indirect techniques. Direct techniques include procedures that directly study liquid-gas two-phase flow in flow channels. Methods such as visualizing a transparent cell [9,10,11], neutron imaging [12,13], X-ray microtomography [14,15], or gas chromatography [16,17] fall into this category.

The indirect study of the liquid-gas two-phase flow in PEM fuel cell flow channels, on the other hand, can be achieved by studying the properties that are the immediate consequence of the liquid water accumulation within flow channels. The two-phase flow pressure drop along the gas channel, for instance, is a property that can describe the amount of liquid water within the flow channels. This property can be considered as an in-situ diagnostic tool that reveals useful information about the amount of liquid water within the gas channel.

## 1.1. Two-Phase Flow Patterns in Minichannels

Liquid-gas two-phase flow is a common form of flow in many industrial applications such as fuel cells, heat exchangers, condensers, chemical processing plants, and air conditioning. However, the two-phase flow in minichannels (hydraulic diameter between  $200\mu\text{m}$  to  $3\text{mm}$ , as categorized by Kandlikar [18]) is considerably different from two-phase flow in conventional channels, i.e. channels with hydraulic diameters greater than  $3\text{mm}$ . This is because viscous stress ( $\sim \mu u/d$ ) and interfacial stress ( $\sim \sigma/d$ ), where  $\sigma$  is surface tension, are more significant than inertial ( $\sim \rho u^2$ ) and gravitational ( $\sim \rho gh$ ) stresses in minichannels. The liquid-gas two-phase flow in minichannels can occur in different patterns such as bubbly flow, slug flow, churn flow, slug-annular flow, and annular flow, as discussed by Triplett et al. [19]. Parameters such as liquid to gas ratio, the superficial velocity of each phase, the surface characteristics of the channel, and the channel geometry, can contribute to this pattern.

Bubbly flow occurs when randomly dispersed bubbles with diameters smaller than the channel diameter occur. For lower superficial liquid velocity, slug flow is observed which includes elongated bubbles. Churn flow is characterized by unstable bubbles or wavy annular flow. Churn flow transits into slug-annular flow for lower liquid flow rates. The slug-annular flow is characterized by wavy-annular flow that does not block the channel. The annular flow occurs when the superficial gas velocity increases and eliminates the wavy form of the slug-annular flow. In PEM fuel cell flow channels, however, bubbly flow does not occur. This is because the superficial liquid velocity in PEM fuel cell flow channels is low. Similarly, churn flow does not occur in PEM fuel cell flow channels as it requires a high liquid to gas ratio.

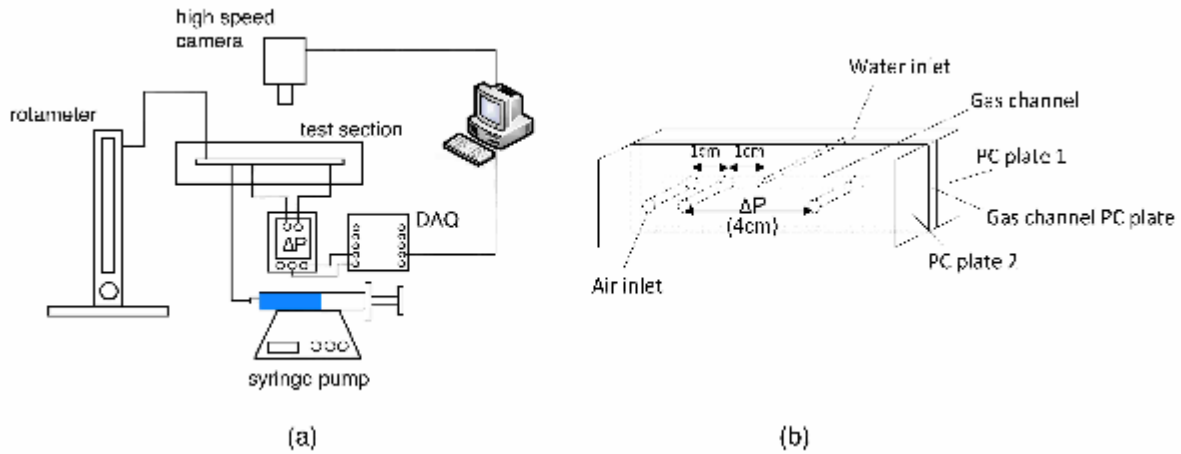


Fig. 1: (a) Experimental setup and (b) test section.

## 1.2. Two-phase flow pressure drop

Despite the single-phase pressure drop which is well identified, the liquid-gas two-phase flow pressure drop is not thoroughly identified. The two-phase flow pressure drop has been studied over a limited range of operating conditions relevant to some particular applications. The physics behind this type of flow is too complicated to be modeled with simplified mathematical expressions. Therefore in most of the published works the two-phase flow pressure drop correlations are improved by correlating experimental results.

The two-phase flow pressure drop is the sum of frictional, gravitational and accelerational pressure drop:

$$\Delta P_{TP} = \Delta P_{TP,F} + \Delta P_{TP,G} + \Delta P_{TP,A} \quad (1)$$

Gravitational pressure drop is a significant term in overall pressure drop in conventional channels. However, the dominant impact of surface tension diminishes the importance of gravitational effects in minichannels. Similarly, for low liquid and gas superficial velocities, the acceleration pressure drop incorporates a small fraction of the overall two-phase flow pressure drop and can be ignored. Therefore the frictional pressure drop becomes the dominant pressure drop term for minichannels in PEM fuel cells.

There are two approaches in identifying the two-phase flow frictional pressure drop. In one approach, the two-phase mixture is treated as a pseudo single phase fluid and properties such as viscosity and density are weighted based on quality. This model is known as the homogeneous equilibrium model and has been reported to be more accurate at higher mass qualities [20,21,22].

In the other method, known as separated flow model, the two-phase pressure drop is related to the single-phase pressure drop through a two-phase flow frictional multiplier,  $\phi^2$ . This method was originally introduced by Lockhart and Martinelli in 1949 [23] and is commonly used for predicting pressure drop in PEM fuel cell flow channels.

In the separated flow model, the two-phase flow pressure drop is correlated to the single phase pressure drop through the two-phase frictional multiplier:

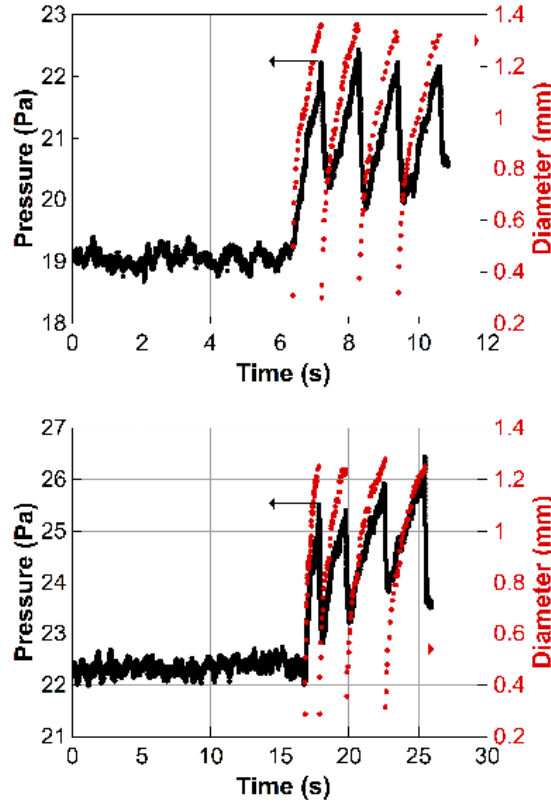


Fig. 2: Two-phase flow pressure drop and droplet diameter, top: superficial air velocity 6.66 m/s and superficial water velocity  $1.205 \times 10^{-4}$  m/s, bottom: superficial air velocity 7.77 m/s and superficial water velocity  $4.639 \times 10^{-5}$  m/s

$$\left(\frac{dP}{dz}\right)_{TP} = \phi_f^2 \left(\frac{dP}{dz}\right)_f \quad (2)$$

where subscripts TP and f represent two-phase and saturated liquid phase, respectively. The Martinelli parameter, X, is defined as:

$$X = \left[ \left(\frac{dP}{dz}\right)_f / \left(\frac{dP}{dz}\right)_g \right]^{\frac{1}{2}} \quad (3)$$

The two-phase frictional multiplier,  $\phi^2$ , is correlated to X and  $X^2$  by Chisholm parameter, C:

$$\phi_f^2 = \frac{\left(\frac{dP}{dz}\right)_{TP}}{\left(\frac{dP}{dz}\right)_f} = 1 + \frac{C}{X} + \frac{1}{X^2} \quad (4)$$

The Chisholm parameter,  $C$ , represents the interaction between liquid and gas phases and depends on the flow regime. The  $C$  values suggested by Chisholm in Ref. [24] are 5 for laminar liquid-laminar gas, 10 for turbulent liquid-laminar gas, 12 for laminar liquid-turbulent gas, and 21 for turbulent liquid-turbulent gas.

Equation 4 originates from the fact that the two-phase flow pressure drop is equal to the sum of the pressure drop for each liquid and gas phase as well as the interaction between them:

$$\left(-\frac{dp}{dz}\right)_{TP} = \left(-\frac{dp}{dz}\right)_f + \left(-\frac{dp}{dz}\right)_g + C \left[ \left(-\frac{dp}{dz}\right)_f \left(-\frac{dp}{dz}\right)_g \right]^{\frac{1}{2}} \quad (5)$$

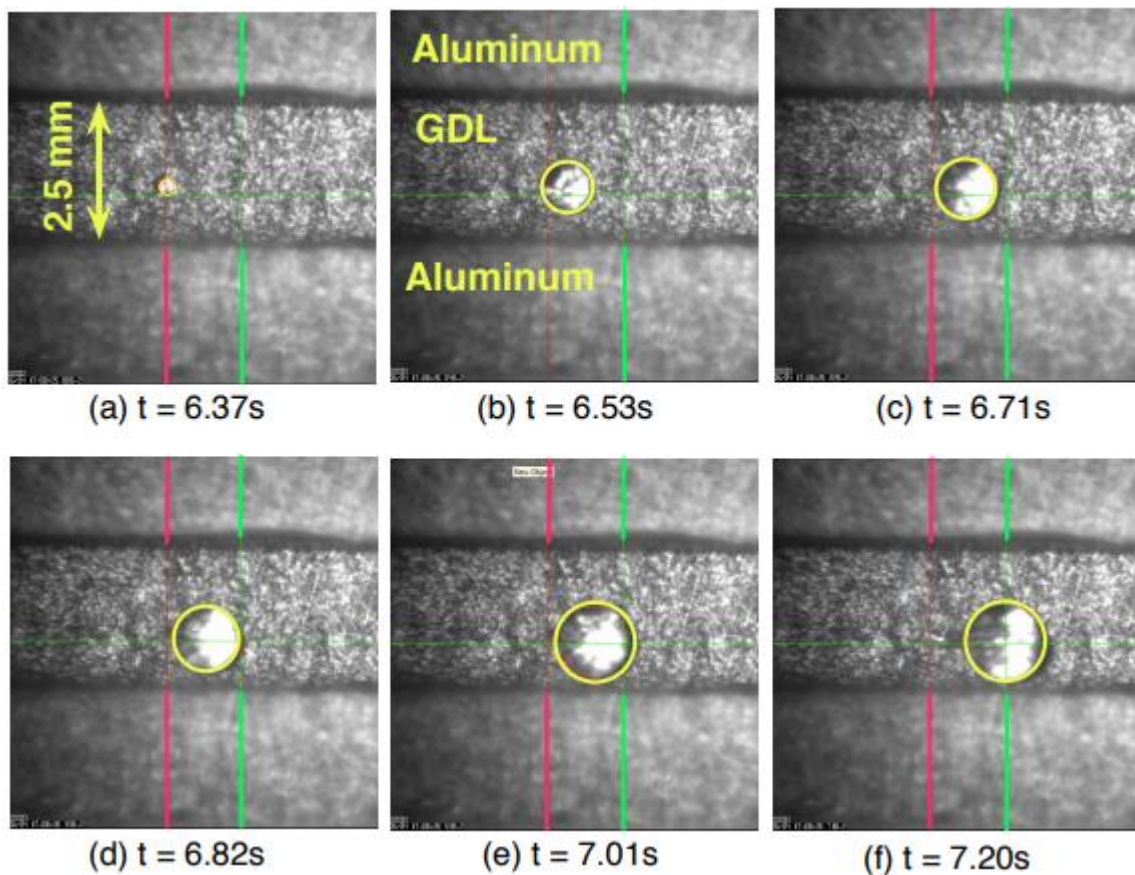


Fig. 3: Droplet images between emergence and detachment. The emergence coordinates are marked with red lines and the detachment coordinates are marked with green lines.

Many researchers have proposed different two-phase flow pressure drop models for conventional channels [25,26,27,28,29,30]. However, such correlations have proven to yield an inferior prediction of two-phase flow pressure drop in microchannels. This is because the surface tension effects are dominant in microchannels while the gravitational force becomes less important. In addition, most of the literature on the topic of two-phase flow pressure drop in minichannels focus on some particular applications such as compact heat exchangers, refrigeration systems, or microtube

condensers. The two-phase flow in PEM fuel cell flow channels is a unique type of flow in microchannels due to different surface energies of the channel walls as well as special liquid water introduction mechanism into the flow channels. Many studies have been conducted to improve Chisholm parameter for a more accurate two-phase flow pressure drop model as reviewed in Ref. [31]. Mishima and Hibiki [32] studied liquid-gas two-phase flow pressure drop in round microchannels with various diameters between 1 mm to 4 mm. It was suggested in their study that the channel diameter should be considered in the C correlation. For circular channels, they proposed that the Chisholm parameter to be calculated by the following equation:

$$C = 21(1 - e^{-0.333D}) \quad (6)$$

where D is the channel diameter in meters. For rectangular channels, they proposed that the Chisholm parameter to be obtained by the following equation:

$$C = 21(1 - e^{-0.319D_h}) \quad (7)$$

where  $D_h$  is the hydraulic diameter.

English and Kandlikar [22] conducted two-phase flow pressure drop experiments in minichannels and improved the Chisholm correlation proposed by Mishima and Hibiki. In their proposed correlation, the numerical coefficient in Eq. 6 and Eq. 7 was replaced with the laminar liquid-laminar gas Chisholm parameter, 5. For circular channels, they proposed:

$$C = 5(1 - e^{-0.333D}) \quad (8)$$

and for rectangular channels they proposed:

$$C = 5(1 - e^{-0.319D_h}) \quad (9)$$

In this study, liquid-gas two-phase flow pressure drop is measured in an ex-situ test PEM fuel cell flow channel while the droplet emergence and growth is captured by a high speed camera. Different air flow rates and liquid water injection rates are employed to collect two-phase flow pressure drop data. The pressure drop data is then utilized along with the droplet size in order to analyze the existing C correlation introduced in Eq. 9.

## 2. Experimental Setup

An ex-situ direct visualization apparatus was designed and fabricated for this study as schematically shown in Figure 1. The test section includes a 2.5mm wide  $\times$  3mm deep gas channel machined on a 3mm thick polycarbonate plate which was sandwiched between two 12.5mm thick polycarbonate plates. The relatively large channel dimensions were chosen such that droplet emergence and transport could be studied in the absence of sidewall effects. GDL sample was inserted between polycarbonate plate 1 and gas channel. Deionized water was injected to the surface of the GDL, on polycarbonate plate 1 side, and was emerged on the surface of the GDL on the other side. The water injection was done through a capillary tube with an inside diameter of 250 $\mu$ m and outside diameter meter of 3.1mm (U 111, Upchurch). Air was supplied into the gas channel through a rotameter (Omega FL 3804ST). Liquid-gas two-phase flow pressure drop was measured within 4cm of the channel with a high accuracy pressure transducer (Omega, PX653-0.25D5V). The pressure transducer could measure 0 to 62Pa pressure (0.25" water) and was used at 1000Hz sampling frequency. Six 1/8 inch screws tightened the whole assembly together. A high speed camera (50KD2B2, Mega Speed) recorded the droplet emergence, growth, and detachment at 100 frames per second speed. In order to avoid air and/or water leakage to the outside, a groove was machined on the polycarbonate plate 1 around GDL location and an o-ring was inserted into it. Figure 1 shows the schematic of the test section and Table 1 lists the experimental conditions.

Toray carbon papers (TGP 060) with a manufacturer-specified thickness of 190 $\mu$ m and 76% porosity was used as the GDL. Toray carbon papers were treated with PTFE based on the procedure presented in Ref. [33]. In this procedure the substrate was dipped in PTFE emulsion (60%wt. dispersion in H<sub>2</sub>O, ALDRICH) for 10 h in order to absorb PTFE

particles. The substrate was then dried at 120°C for 1 hour. In next step, the temperature of the furnace was increased to 360°C for 1 hour. The PTFE weight percent loaded on the GDL was controlled by the PTFE concentration in the emulsion. The superficial gas velocity in table 1 is calculated based on the bulk velocity of gas flowing within the channel cross sectional area. Similarly, superficial water velocity was calculated based on water volumetric flow rate passing through the gas channel:

$$\text{superficial gas velocity} = \frac{\text{air flow rate}}{\text{gas channel cross sectional area}} \quad (10)$$

$$\text{superficial water velocity} = \frac{\text{water injection rate}}{\text{gas channel cross sectional area}} \quad (11)$$

### 3. Results and Discussion

#### 3.1. Two-Phase Flow Pressure Drop

Liquid water droplet emergence and growth was recorded with a high speed camera and liquid-gas two-phase flow pressure drop was measured simultaneously. Figure 2 shows the droplet size and two-phase flow pressure drop for two superficial air velocities of 6.66m/s and 7.77m/s with 1163 and 1357 air Reynolds numbers, respectively. Comparison between different superficial air velocities in Figure 2 shows that for higher superficial air velocity droplets detach at smaller diameters and the two-phase flow pressure drop is greater. This is because the higher superficial air velocity causes more drag force on the emerging droplet. For 6.66m/s superficial gas velocity the single gas phase flows within the gas channel until  $t = 6.3\text{s}$  at which the first droplet emerges from the surface of the GDL. By emerging the first droplet, the single gas

Table 1: Experimental conditions.

Air flow rate (mℓ/min)	Superficial air velocity(m/s)	Air Reynolds number	Water flow rate (μℓ/h)	Superficial water velocity (m/s)	Water Reynolds number
2400	5.33	903.9	1859	$6.883 \times 10^{-5}$	0.186
2700	6	1047.3	2200	$8.14 \times 10^{-5}$	0.220
3000	6.66	1163.6	3255	$1.205 \times 10^{-4}$	0.326
3250	7.22	1260.6	3255	$1.205 \times 10^{-4}$	0.326
3500	7.77	1357.6	1253	$4.639 \times 10^{-5}$	0.125

phase flow changes into two-phase flow within the flow channel and the pressure drop starts to increase. Droplet images at six different time intervals are shown in Figure 3. The red lines on images show droplet emergence coordinate and the green lines show droplet detachment coordinate. The pressure drop increases until  $t = 7.2\text{s}$  where the first droplet detaches from the surface of the GDL. At  $t = 6.8\text{s}$  a change in pressure profile and droplet size data is observed which can be due to droplet's temporary displacement on the GDL surface. For superficial air velocity of 6.66 m/s the average two-phase flow pressure drop measured at droplet detachment is 22.20 Pa and the predicted two-phase pressure drop based on C value obtained from Eq. 9 is 20.6 Pa. For superficial air velocity of 7.77 m/s the average two-phase flow pressure drop measured at droplet detachment is 25.2 Pa and the predicted two-phase flow pressure drop based on same equation is 23.3 Pa. This indicates that Eq. 9 can predict the two-phase flow pressure drop within 10% of accuracy for these two cases. However, a wider range of experimental conditions should be tested for validity of this equation for PEM fuel cell application.

The experimentally measured two-phase flow pressure drop can be used to back calculate the C value in Eq. 4. Figure 4 shows the back calculated C values during droplet growth. Figure 4 also shows the C parameter calculated from Eq. 9. It can be observed that for both superficial air velocities, the back calculated C value at droplet detachment is significantly greater than the C value obtained from Equation 9. For superficial air velocity of 6.66m/s the average value of back calculated C parameter is 3.30 with a standard deviation of 1.33. However, for higher superficial air velocity, 7.77 m/s, most of the back calculated C values are greater than the C value obtained from Eq. 9. For this superficial air velocity, the

average C value is 6.05 with a standard deviation of 2.11. The C value obtained from Eq. 9 is 2.90 for the gas channel used in this study.

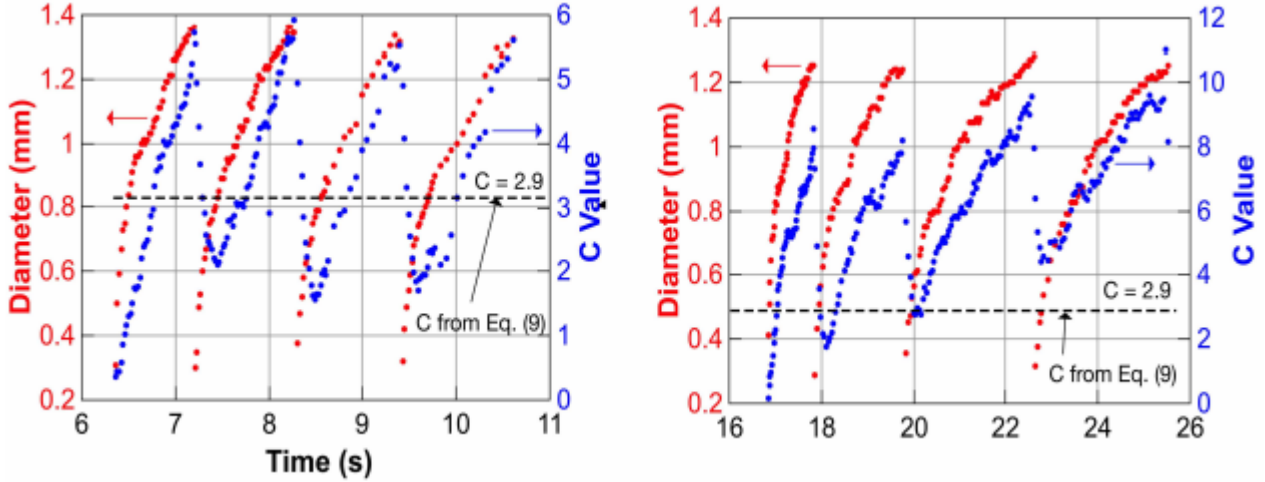


Fig. 4: Droplet diameter (red) and back calculated C values (blue), top: superficial air velocity 6.66 m/s and superficial water velocity  $1.205^{-4}$  m/s, bottom: superficial air velocity 7.77 m/s and superficial water velocity  $4.639^{-5}$  m/s.

### 3.2. Drag coefficient

The two-phase flow pressure drop data and droplet size during its growth can be utilized to find the drag force applied on the droplet. For an inertial control volume, the linear momentum equation is given as:

$$\frac{\partial}{\partial t} \int_{CV} \mathbf{V} \rho dV + \int_{CS} \mathbf{V} \rho \mathbf{V} \cdot \mathbf{n} dA = \Sigma \mathbf{F} \quad (12)$$

For single-gas flow passing through a gas channel at steady state, the first term on Eq. 12 is zero and therefore the friction force exerted by the channel wall can be obtained according to the second term on the left hand side:

$$\Delta P_{\text{single phase}} \times A_{\text{channel wall}} = \text{Frictional force from walls} \quad (13)$$

As water droplet emerges from the GDL surface, drag force should be considered on the right hand side of the equation:

$$\Delta P_{\text{single phase}} \times A_{\text{channel wall}} + \Delta P_{\text{increase in pressure}} \times A_{\text{projected}} = \text{Frictional force from walls} + \text{Drag force} \quad (14)$$

where  $A_{\text{projected}}$  is the droplet's projected area normal to the gas flow direction. By subtracting Eq. 13 from Eq. 14, one can find the drag force,  $F_D$ :

$$\Delta P_{\text{increase in pressure}} \times A_{\text{projected}} = \text{Drag force} \quad (15)$$

$$F_D = \rho A_{\text{projected}} V^2 C_D \quad (16)$$

where  $V$  is the superficial air velocity and  $C_D$  is the drag coefficient. The drag coefficients calculated for different superficial air velocities are shown in Figure 5. It can be observed that drag coefficient decreases over time. This is because as droplet grows in size, the projected area in drag force equation, Eq. 16, becomes more dominant and drag coefficient decreases to compensate for relatively small drag force addition over time.

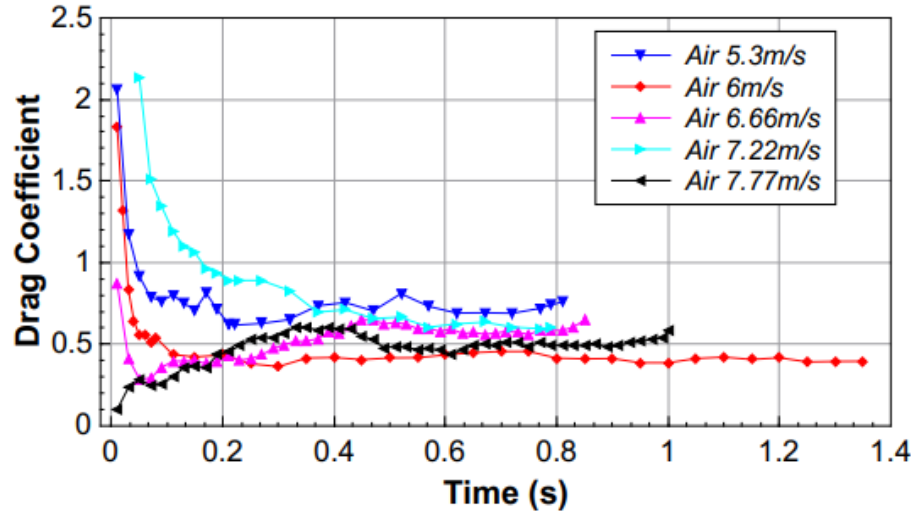


Fig. 5: Drag coefficient for different superficial air velocities.

It should be added in order to find  $A_{\text{projected}}$ , droplet's sessile contact angle on GDL sample was used. This contact angle had been previously measured and obtained by authors in Ref. [34,35, 36].

#### 4. Conclusion

The interaction between liquid water droplet growth and two-phase flow pressure drop in an ex-situ PEM fuel cell test section was studied. The following conclusions can be drawn from this study:

1. Droplets detach at smaller diameter as the superficial air velocity in flow channel increases. This is because increasing gas flow rate increases the drag force applied on the droplet and can detach it at a smaller projected area.
2. As water droplet is introduced in the gas channel, the pressure drop increases. This increased pressure drop can be used as an in-situ diagnostic tool that reveals information about the amount of water within flow channel.
3. It was observed in this study that as droplet detaches from the GDL surface, the pressure drop along the gas channel decreases. This is because the detached droplet exits the length of the flow channel in which pressure measurement was conducted. In an actual fuel cell, however, the detached water droplets may remain within fuel cell assembly and still cause two-phase flow pressure drop.
4. It was observed that the C correlation proposed by English and Kandlikar can properly predict the two-phase flow pressure drop for the experimental conditions used in this study.
5. The comparison between two-phase flow pressure drop and single-phase gas flow pressure drop was utilized to calculate the drag coefficient of the emerging droplets.

#### Acknowledgments

Michigan Technological University is gratefully acknowledged for providing the startup fund for this study.

#### References

- [1] A. Faghri, Z. Guo, "Challenges and Opportunities of Thermal Management Issues Related to Fuel Cell Technology and Modeling," *Int. J. Heat Mass Transfer*, 2005.
- [2] A. Appleby, "Issues in fuel cell commercialization," *J. Power Sources*, pp.153-176, 1996.
- [3] G. Park, Y. Sohn, T. Yang, Y. Yoon, W. Lee, C. Kim, "Effect of PTFE contents in the gas diffusion media on the performance of PEMFC," *J. Power Sources*, pp. 182-187, 2004.
- [4] J. Itonen, M. Mikkola, G. Lindbergh, "Flooding of gas diffusion backing in PEFCs physical and electrochemical characterization," *Journal of the Electrochemical Society*, pp. A1152-A1161, 2004.
- [5] U. Pasaogullari, C. Y. Wang, "Liquid water transport in gas diffusion layer of polymer electrolyte fuel cells," *J. Electrochem. Soc.*, 2004.

- [6] A. Bazylak, D. Sinton, N. Djilali, "Dynamic water transport and droplet emergence in PEMFC gas diffusion layers," *J. Power Sources*, pp. 240-246, 2008.
- [7] X. Liu, H. Guo, C. Ma, "Water flooding and two-phase flow in cathode channels of proton exchange membrane fuel cells," *J. Power Sources*, pp. 267-280, 2006.
- [8] I. Hussaini, C. Y. Wang, "Visualization and quantification of cathode channel flooding in PEM fuel cells," *J. Power Sources*, pp. 444-451, 2009.
- [9] F. Zhang, X. Yang, C. Y. Wang, "Liquid Water Removal From A Polymer Electrolyte Fuel Cell," *J. Electrochem. Soc.*, 2006.
- [10] T. Klaus, D. Pocza, H. Christopher, "Visualization of water buildup in the cathode of a transparent PEM fuel cell," *J. Power Sources* pp. 403-414, 2003.
- [11] D. Spornjak, A. Prasad, S. Advani, "Experimental investigation of liquid water formation and transport in a transparent single serpentine PEM fuel cell," *J. Power Sources*, pp. 334-344, 2007.
- [12] J. Owejan, T. Trabold, D. Jacobson, M. Arif, S. Kandlikar, "Effects of flow field and diffusion layer properties on water accumulation in a PEM fuel cell," *Int. J. Hydrogen Energy*, pp. 4489-4502, 2007.
- [13] M. Hickner, N. Siegel, K. Chen, D. Hussey, D. Jacobson, M. Arif, "In situ high-resolution neutron radiography of cross-sectional liquid water profiles in proton exchange membrane fuel cells," *J. Electrochem. Soc.*, pp. 427-434, 2008.
- [14] P. Sinha, P. Halleck, C. Y. Wang, "Quantification of liquid water saturation in a PEM fuel cell diffusion medium using X-ray microtomography," *Electrochemical and Solid-State Letters*, pp. 344-348, 2006.
- [15] S. Lee, N. Lim, S. Kim, G. Park, C. Kim, "X-ray imaging of water distribution in a polymer electrolyte fuel cell," *J. Power Sources*, pp. 867-870, 2008.
- [16] M. Mench, Q. Dong, C. Y. Wang, "In situ water distribution measurements in a polymer electrolyte fuel cell," *J. Power Sources*, pp. 90-98, 2003.
- [17] X. Yang, N. Burke, C.Y. Wang, K. Tajiri, K. Shinoharab, "Simultaneous Measurements of Species and Current Distributions in a PEFC under Low-Humidity Operation," *J. Electrochem. Soc.*, pp. 759-766, 2005.
- [18] S. Kandlikar, W. Grande, J. William, "Evolution of Microchannel Flow Passages-Thermohydraulic Performance and Fabrication Technology," *Heat Transfer Engineering*, pp. 3-17, 2003.
- [19] K. Triplett, S. Ghiaasiaan, S. Abdel-Khalik, D. Sadowski, "Gas-liquid two-phase flow in microchannels Part I: two-phase flow patterns," *Int. J. Multiphase Flow*, pp. 377-394, 1999.
- [20] H. Ide, H. Matsumura, "Frictional pressure drops of two-phase gas-liquid flow in rectangular channels," *Experimental Thermal and Fluid Science*, pp. 362-372, 1990.
- [21] M. Grimm, E. See, and S. Kandlikar, "Modeling gas flow in PEMFC channels: Part I—Flow pattern transitions and pressure drop in a simulated ex situ channel with uniform water injection through the GDL," *Int. J. Hydrogen Energy*, pp. 12489-12503, 2012.
- [22] N. English, S. Kandlikar, "An experimental investigation into the effect of surfactants on air-water two-phase flow in minichannels," *Heat transfer engineering*, pp. 99-109, 2006.
- [23] R. W. Lockhart, R. C. Martinelli, "Proposed correlation of data for isothermal two-phase, two-components flow in pipes," *Chemical Engineering Progress*, pp. 38-48, 1949.
- [24] D. Chisholm, "A theoretical basis for the Lockhart-Martinelli correlation for two-phase flow," *Int. J. Heat and Mass*, 1967, pp. 1767- 1778.
- [25] L. Friedel, "Pressure drop during gas vapor liquid flow in pipes," *International Chemical Engineering*, pp. 352-367, 1980.
- [26] H. Muller-Steinhagen, K. Heck, "A simple friction pressure drop correlation for two-phase flow in pipes," *Chemical Engineering and Processing: Process Intensification*, 1986, pp. 297-308.
- [27] S. Saisorn and S. Wongwises, "The effects of channel diameter on flow pattern, void fraction and pressure drop of two phase air water flow in circular micro-channels," *Experimental Thermal and Fluid Science*, pp. 454-462, 2010.
- [28] S. Kim and I Mudawar, "Universal approach to predicting two-phase frictional pressure drop for mini/micro-channel saturated flow boiling," *International Journal of Heat and Mass Transfer*, pp. 718-734, 2013.
- [29] L. Sun, K. Mishima, "Evaluation analysis of prediction methods for two-phase flow pressure drop in mini-channels," *International Journal of Multiphase Flow*, pp. 47-54, 2009.

- [30] G. Ribatski, L. Wojtan, J. Thome, "An analysis of experimental data and prediction methods for two-phase frictional pressure drop and flow boiling heat transfer in micro-scale channels," *Experimental Thermal and Fluid Science*, 2006, pp. 1-19.
- [31] M. Mortazavi, K. Tajiri, "Two-phase flow pressure drop in flow channels of proton exchange membrane fuel cells: Review of experimental approaches," *Renewable and Sustainable Energy Reviews*, pp. 296-317, 2015.
- [32] K. Mishima, T. Hibiki, "Some characteristic of air-water two-phase flow in small diameter vertical tubes," *Int. J. Multiphase Flow*, pp. 703-712, 1996.
- [33] C. Hwang, M. Ishida, H. Ito, T. Maeda, A. Nakano, Y. Hasegawa, N. Yokoi, A. Kato, T. Yoshida, "Influence of properties of gas diffusion layers on the performance of polymer electrolyte-based unitized reversible fuel cells," *Int. J. Hydrogen Energy*, pp. 1740-1753, 2010.
- [34] M. Mortazavi and K. Tajiri, "Liquid water breakthrough pressure through gas diffusion layer of proton exchange membrane fuel cell," *Int. J. Hydrogen Energy*, 2014, pp. 9409-9419.
- [35] M. Mortazavi and K. Tajiri, "Effect of the PTFE content in the gas diffusion layer on water transport in polymer electrolyte fuel cells (PEFCs)," *J. Power Sources*, 2014, pp. 236-244.
- [36] M. Mortazavi and K. Tajiri, "In-Plane Microstructure of Gas Diffusion Layers With Different Properties for PEFC," *ASME Journal of Fuel Cell Science and Technology*, vol. 11, 2014.